

Constraining the primordial power spectrum from SNIa lensing dispersion

Ido Ben-Dayan¹, Tigran Kalaydzhyan²

¹*Deutsches Elektronen-Synchrotron DESY, Theory Group, D-22603 Hamburg, Germany and*

²*Department of Physics and Astronomy, Stony Brook University,
Stony Brook, New York 11794-3800, USA*

The (absence of detecting) lensing dispersion of Supernovae type Ia (SNIa) can be used as a novel and extremely efficient probe of cosmology. In this preliminary example we analyze its consequences for the primordial power spectrum. The main setback is the knowledge of the power spectrum in the non-linear regime, $1 \text{ Mpc}^{-1} \lesssim k \lesssim 10^2 - 10^3 \text{ Mpc}^{-1}$ at redshift of about unity. By using the lensing dispersion and conservative estimates in this regime of wavenumbers, we show how the current upper bound $\sigma_\mu(z=1) < 0.12$ on *existing data* gives strong indirect constraints on the primordial power spectrum. The probe extends our handle on the spectrum to a total of 12 – 15 inflation e-folds. These constraints are so strong that they are already ruling out a large portion of the parameter space allowed by PLANCK for running $\alpha \equiv dn_s/d\ln k$ and running of running $\beta \equiv d^2n_s/d\ln k^2$. The bounds follow a linear relation to a very good accuracy. A conservative bound disfavors any enhancement above the line $\beta(k_0) = 0.032 - 0.41 \alpha(k_0)$ and a realistic estimate disfavors any enhancement above the line $\beta(k_0) = 0.019 - 0.45 \alpha(k_0)$.

PACS numbers: 98.80.-k, 98.62.Sb, 98.80.Cq

Introduction: Cosmology is becoming a precise science, most notably due to increasing number and quality of measurements. Utilizing several probes is crucial in breaking degeneracies between cosmological parameters. The combination of CMB, large scale structure (LSS) and Type Ia Supernovae (SNIa) has lead to the emergence of the “concordance model” of cosmology. The SNIa owe their success to the small intrinsic dispersion around their mean luminosity. By observing supernovae at cosmological distances, we can measure the luminosity-redshift relation $d_L(z)$ and infer cosmological parameters from the mean luminosity. However, the intrinsic dispersion of SNIa luminosities is not the only source of scatter in the data. Photons arriving from these ‘Standard Candles’ are affected by the inhomogeneous matter distribution between the source and observer. This induces an additional scatter in the luminosity-redshift relation, making it a *stochastic* observable with mean, dispersion, etc. Therefore, by disentangling this cosmic dispersion from the intrinsic scatter, we can potentially probe background parameters like Ω_{m0} or fluctuations, i.e. the *power spectrum*. Our main interest will be the lensing contribution, dominating at $z \gtrsim 0.3$.

We suggest to use the lensing dispersion of SNIa as an additional probe of cosmology. The now operational Dark Energy Survey [2] will measure thousands of SNIa, up to redshift $z \sim 1.2$ and LSST [3] will measure millions of SNIa. This will reduce statistical errors considerably and increase the chance for detection since the lensing dispersion grows with the redshift at $z \sim 1$ [4–6]. With future data, it has been suggested to use the lensing dispersion to constrain the present matter density Ω_{m0} and σ_8 [4, 7, 8].

In this preliminary note we analyze the implications of

the lensing dispersion σ_μ on the primordial power spectrum. The distance modulus,

$$\mu = 5 \log_{10} \left(\frac{d_L(z)}{10 \text{ pc}} \right), \quad (1)$$

is a function of the luminosity distance $d_L(z)$ to the source at redshift z . Existing data analysis has not detected lensing dispersion with enough statistical significance, but has placed an upper bound of $\sigma_\mu \leq 0.12$ for the redshift of up to unity [9–13] at 95% CL.

In principle, the primordial power spectrum is not limited to a specific parameterization. In practice, the primordial power spectrum is typically parametrized as $P_k = A_s (k/k_0)^{n_s(k_0)-1}$, where k_0 is a suitable “pivot scale”. A common, more general form, is when the spectral index $n_s(k)$ is scale dependent, and then expanded around the pivot scale k_0 ,

$$P_k = A_s \left(\frac{k}{k_0} \right)^{n_s(k_0) - 1 + \frac{\alpha(k_0)}{2} \ln \frac{k}{k_0} + \frac{\beta(k_0)}{6} \ln^2 \frac{k}{k_0}}, \quad (2)$$

where α is typically dubbed the “running” of the spectral index, and β , the “running of running”. The best constraints on α, β with $k_0 = 0.05 \text{ Mpc}^{-1}$, $n_s(k_0) \simeq 0.96$ are given by PLANCK [1]. More generally, CMB and LSS observations only give a direct measurement for wave numbers in the range $H_0 \leq k \lesssim 1 \text{ Mpc}^{-1}$. In terms of inflation, the direct measurement of $k \lesssim 1 \text{ Mpc}^{-1}$ corresponds to about 8 e-folds of inflation, leaving most of the

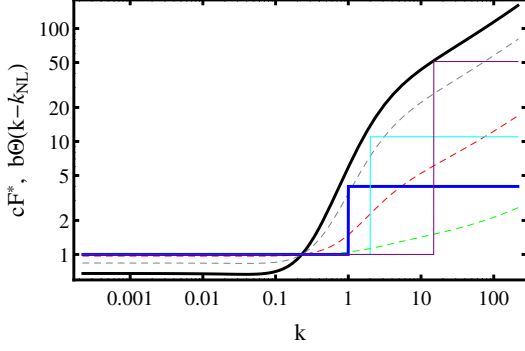


FIG. 1: Log-Log plot of the “transfer functions” (9) at redshift $z = 1$, $z^* = 0.5$ multiplied by $c = 1$ (solid black), $c = 0.5$ (dashed grey), $c = 0.1$ (dashed red) $c = 0.01$ (dashed green). Solid blue, cyan and purple curves are the step functions in (10) with $b = 3$, $k_{NL} = 1 \text{ Mpc}^{-1}$; $b = 10$, $k_{NL} = 2 \text{ Mpc}^{-1}$; $b = 50$, $k_{NL} = 15 \text{ Mpc}^{-1}$, respectively.

power spectrum of ~ 60 e-folds out of reach¹. Therefore, even after PLANCK there is still an enormous space of inflationary models allowed. It is therefore of crucial importance to infer as much of the spectrum as possible to rule out chunks of models, and single out preferred ones. Due to Silk damping, beyond the scale of $k \lesssim 1 \text{ Mpc}^{-1}$, CMB anisotropies stop being a useful probe. Instead, we have indirect bounds such as the absence of primordial black holes and Ultracompact Minihalos or prospects of measuring spectral distortions of the CMB blackbody spectrum [14–19] with PIXIE/PRISM [20, 21]. Consideration of the lensing dispersion, gives access to 2–3 more decades of the spectrum, because the dispersion involves an integral over the power spectrum, see below. These 2–3 decades correspond to additional 4–7 e-folds, yielding a total of 12–15 e-folds. Albeit degenerate with other cosmological parameters, it surpasses the previous methods by actually cutting into the allowed parameter space allowed by PLANCK, using *existing data* only. In a separate publication [22], we analyze the case where the power spectrum takes a different “non-slow-roll” parameterization such as in cases analyzed in [18].

Method: We start from the full dispersion expression of the luminosity distance, calculated in the light-cone average approach up to second order in the Poisson (longitudinal) gauge, [6, 23–26], and recently confirmed in [27]. The dominant contribution of the dispersion at $z \gtrsim 0.3$, comes from the lensing contribution. For ΛCDM this has been computed to a good approximation:

$$\sigma_\mu(z) = \frac{2.5}{\ln 10} \sqrt{\int \frac{d\Omega}{4\pi} \int_{\eta_s^{(0)}}^{\eta_o} \prod_{i=1}^2 \frac{d\eta_i}{\Delta\eta} \frac{\eta_i - \eta_s^{(0)}}{\eta_o - \eta_i} \Delta_2 \Psi|_{r_i=\eta_o-\eta_i}}, \quad (3)$$

where η_o is the observer conformal time and $\eta_s^{(0)}$ is the conformal time of the source with unperturbed geometry, see [6] for technical terms and explanations. Considering the ensemble and light-cone average then give:

$$\begin{aligned} \sigma_\mu(z) &\simeq \frac{5}{\ln 10} \sqrt{\int \frac{dk}{k} P_\Psi(k, \eta(z)) \frac{(k\Delta\eta(z))^3}{15} Si(k\Delta\eta(z))} \\ &\simeq 0.7 \sqrt{\int \frac{dk}{k} P_\Psi(k, z) \left(\frac{k}{H_0}\right)^3 \tilde{\Delta}\eta(z)^3}, \end{aligned} \quad (4)$$

where $\Delta\eta = \eta_s^{(0)} - \eta_o \equiv \tilde{\Delta}\eta/H_0$, $Si(x) = \int_0^x \frac{\sin q}{q} dq$,

$$\tilde{\Delta}\eta(z) = \int_0^z \frac{dy}{\sqrt{\Omega_{m0}(1+y)^3 + \Omega_{\Lambda 0}}}, \quad (5)$$

and P_Ψ is the linear or non-linear power spectrum of the *gravitational potential*². We will be mostly interested in the dispersion at $z = 1$ where sufficient data is available and because up to the redshift of a few, the dispersion grows approximately linearly [6, 12, 13, 28], so the best constraints can be given at the maximal available redshift. Substituting $z = 1$, and PLANCK most likelihood values of $H_0, \Omega_{m0}, \Omega_{\Lambda 0}$ gives:

$$\sigma_\mu(z=1) \simeq 0.47 \sqrt{\int dk k^2 P_\Psi(k, 1)} \equiv 0.47 \sqrt{T_2(P)} \quad (6)$$

in the linear case. As discussed in [6], one can treat the complicated numerical integrals over redshift and wavenumber of the non-linear power spectrum efficiently and to an accuracy of $\sim 10\%$ if one substitutes $P_\Psi(k, z) \simeq (g(z)/g(z^*))^2 P_\Psi(k, z^*)$, where $g \simeq \frac{5}{2} g_\infty \Omega_m \left\{ \Omega_m^{4/7} - \Omega_\Lambda + (1 + \Omega_m/2)(1 + \Omega_\Lambda/70) \right\}^{-1}$ is the so-called linear growth factor and $z^* = z/2$, but it is not particularly sensitive to that choice. The corresponding dispersion in this case will be

$$\sigma_\mu^*(z=1) \simeq 0.49 \sqrt{\int dk k^2 P_\Psi^*(k, 0.5)} \equiv 0.49 \sqrt{T_2^*(P)} \quad (7)$$

¹ In principle, it is possible that primordial perturbations have been generated only during these 8 e-folds. However, to solve the homogeneity and horizon problem, one usually requires about 60 or at least several tens of e-folds. Shutting down the generation of perturbations during these e-folds is rather tuned.

² A similar formula can be derived for any perturbed FLRW cosmology in which photons fulfill the geodesic equations of general relativity, such as dark energy models. The only change is the time dependent behaviour of the gravitational potential Ψ .

We shall use both estimates σ_μ, σ_μ^* .

Hence, the lensing dispersion of supernovae is a direct measurement of the integrated late-time power spectrum. Given the bound $\sigma_\mu < 0.12$ gives the prediction that the second moment of the power spectrum at $z = 1$ is at most $T_2(P) \equiv \int dk k^2 P_\Psi(k, 1) \lesssim 0.065$. At the most basic level, this can be used to constrain parameterizations of the late-time power spectrum, or cosmological parameters such as Ω_{m0}, σ_8 or $w(z)$. The k^2 enhancement, makes it a much more sensitive probe to small scales of the power spectrum than σ_8 .

Assuming the standard Λ CDM evolution the dispersion probes the primordial power spectrum. There is of course a degeneracy between the power spectrum and cosmological parameters such as $H_0, \Omega_{m0}, \Omega_{\Lambda 0}$ or even $w(z)$, and a full statistical analysis is necessary. This is beyond the scope of this paper, but the current parameters are rather well constrained already to the order of 10%, and their effect on the final outcome is limited to that³. Here we simply take PLANCK's maximal likelihood values for them in the presence of non-zero running $\alpha(k_0)$ and "running of running", $\beta(k_0)$.

The above formula for the dispersion is both IR and UV finite. Modes with $k \leq H_0$ are obviously subdominant because of the $(k/H_0)^3$ factor so we neglect them. On the UV tail, the dispersion converges as long as the spectrum decays at least as k^ν , $\nu < -3$. To the best of our knowledge, all simulations or analytical considerations fulfill this condition. The main limitation is, therefore, the validity of the spectrum, and there is some sensitivity to the actual cut-off taken. For $k \gg H_0$ at some redshift dependent point standard cosmological perturbation theory breaks down, and one has to resort to numerical simulations to get an approximate fitting formula for the power spectrum, like the HaloFit model, [29–31]. The fitting formula reaches $k_{UV} = 30h \text{ Mpc}^{-1}$ with 10% accuracy and $k_{UV} = 320h \text{ Mpc}^{-1}$, where accuracy drops to 20%. The dispersion with $k_{UV} = 30h \text{ Mpc}^{-1}$ is about 15% smaller than $k_{UV} = 320h \text{ Mpc}^{-1}$ and integrating out to infinity only induces additional 10% enhancement. Therefore we take $k_{UV} = 320h \text{ Mpc}^{-1}$ as our UV cut-off, and our results are accurate to about 20%. Considering enough running, or running of running, the HaloFit fitting formula stops being useful because it is sensitive to the initial conditions. It is nevertheless obvious that the non-linear evolution causes clustering and enhances the power spectrum. For example, at redshift $z = 1$, the ratio between the HaloFit formula, $P_{NL}(k, z)$, with standard initial conditions ($n_s \simeq 0.96$, $\alpha = \beta = 0$) and the linear power spectrum $P_L(k, z^*)(g(z)/g(z^*))^2/P_L(k, z)$ is the solid, thick, black curve plotted in Fig. 1. Already at

$k = 1 \text{ Mpc}^{-1}$ the non-linear power spectrum is a factor of a few larger than the linear one, and for $k \gtrsim 10 \text{ Mpc}^{-1}$, it behaves as a power law with a scaling exponent of nearly 1/2. We therefore utilize this ratio in the standard case of $n_s = \text{const.}$ to define a "transfer function",

$$F(k, z) \equiv \frac{P_{NL}(k, z)}{P_L(k, z)}, \quad (8)$$

$$F^*(k, z, z^*) \equiv \frac{P_{NL}(k, z^*)(g(z)/g(z^*))^2}{P_L(k, z)}, \quad (9)$$

where P_{NL} is the non-linear power spectrum, $P_L = (3/5)^2 P_k T^2(k) g^2(z)$ is the linear spectrum and $T(k)$ is the Eisenstein and Hu transfer function with baryons [32], all taken in the standard scenario with $n_s \simeq 0.96, \alpha = \beta = 0$. We take the enhancement into account in two simple ways. The first method is by a Heaviside function $\Theta(k)$. Here we are not limited to the HaloFit formula, so we can use $T_2(P)$:

$$T_2(P) = \int_{H_0}^{k_{UV}} dk k^2 P_L(1 + b \Theta(k - k_{NL})), \quad (10)$$

and we evaluate $T_2(P)$ for $b = 0, 3, 10, 50$ with corresponding $k_{NL} = 1, 1, 2, 15 \text{ Mpc}^{-1}$, at $z = 1$, such that the step function is always underestimating the transfer function F^* . At $z = 1, z^* = 0.5$, $F^*(k, z, z^*) < F(k, z)$ so using only steps smaller than F^* is an even more conservative estimate. The step functions are the solid blue, cyan and purple lines in Fig. 1. The second method, is by using F^* of the HaloFit model, such that

$$T_2^*(P) = \int_{H_0}^{k_{UV}} dk k^2 P_L(k)(1 - c + c F^*(k, z, z^*)), \quad (11)$$

Again we will evaluate $T_2^*(P)$ at $z = 1, z^* = 0.5$. In both methods $b = 0$ or $c = 0$ correspond to computing the dispersion with the linear power spectrum only.

$c = 1$ corresponds to exactly following the HaloFit enhancement pattern. Except $c = 1$ all the second method values of c are underestimates as well. The resulting enhancement is plotted in Fig. 1 as green, red and grey dashed lines.

Results: In Fig. 2 we show the constraints on running and running of running from the non-detection of lensing dispersion overlaid on PLANCK likelihood contours. In the left panel, the values $b = 0, 3, 10, 50$ with corresponding $k_{NL} = 1, 1, 2, 15 \text{ Mpc}^{-1}$ are considered. The right panel considers $c = 0, 0.01, 0.1, 0.5, 1$. In both panels, coloured regions give $\sigma_\mu \geq 0.12$ and are disfavoured. We expect that simulations with initial conditions that include non-zero α, β will give result similar to the latter case of $c = 1$.

We wish to note that there are additional factors which make our analysis an underestimate. First of all, the light-cone average is integrating over the whole sky (2-sphere, at fixed redshift on the past light-cone). Partial

³ For example, WMAP9 most likelihood values give a 10% smaller $\sigma_\mu(z = 1) = 0.077$ than PLANCK $\sigma_\mu(z = 1) = 0.085$.

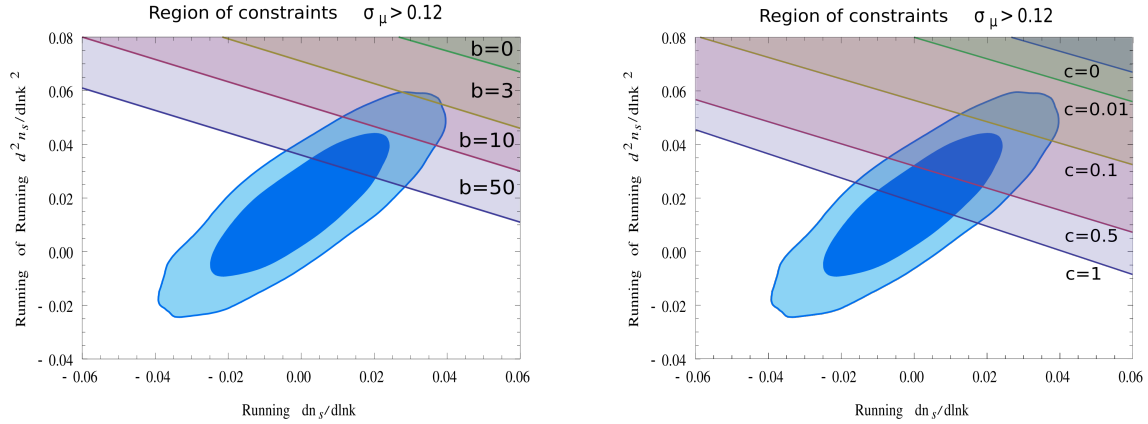


FIG. 2: Regions of allowed parameters combined with PLANCK data. The ellipses are the 68% and 95% CL contours from [1]. In the coloured regions $\sigma_\mu > 0.12$ and are disfavoured for $b = 0, 1, 3, 10, 50$ (right panel) and $c = 0, 0.01, 0.1, 0.5, 1$ (left panel)

sky coverage is expected to increase dispersion [5]. Second, the bound $\sigma_\mu \leq 0.12$ in some analyses refers to the total dispersion, which includes additional contributions such as intrinsic dispersion, that might actually dominate the dispersion. Third, SNIa at higher redshift have already been detected and used for cosmological parameter inference. The monotonicity of $\sigma_\mu(z)$ ensures that considering, for instance, $\sigma_\mu(z = 1.2)$, would have given even more stringent bounds.

Conclusions and Outlook: From Fig. 2, it is obvious that the lensing dispersion, or its absence is an extremely powerful cosmological probe. Even if a scale dependent spectral index induces clustering which is *an order of magnitude smaller* than the standard constant n_s scenario, some of the parameter space allowed by PLANCK is ruled out. Moreover, the analysis discusses the spectrum up to $k \sim 320h \text{ Mpc}^{-1}$, more than two orders of magnitude beyond PLANCK's lever arm (~ 5 e-folds more) irrespective of whether models are ruled in or out. It can be treated as a prediction of inflationary models. In the more realistic case where the enhancement is similar to the HaloFit model, such as $c = 0.5, 1$ or $b = 50$ one gets strong bounds on the allowed parameters, that can be expressed as a linear relation:

$$\beta(k_0) \leq 0.036 - 0.42 \alpha(k_0), \quad b = 50 \quad (12)$$

$$\beta(k_0) \leq 0.032 - 0.41 \alpha(k_0), \quad c = 0.5 \quad (13)$$

$$\beta(k_0) \leq 0.019 - 0.45 \alpha(k_0), \quad c = 1 \quad (14)$$

Allowing $\alpha, \beta \neq 0$, PLANCK got $\alpha(k_0) = 0^{+0.016}_{-0.013}$ and $\beta(k_0) = 0.017^{+0.016}_{-0.014}$. This results nicely matches the realistic case of $\beta(k_0) \leq 0.019$. Any improvement such as reducing the bound to $\sigma_\mu \leq 0.1$, or reducing the error bars will obviously tighten the constraints. In fact, all analyses (data, statistical, theoretical and numerical) [6, 11–13, 28, 33] point to a lower value of the dispersion, at most $\sigma_\mu \simeq 0.093z$, practically disfavoring even a larger portion of the parameter space allowed by

PLANCK. This will really turn the lensing signal into a cosmological probe, similar to CMB lensing.

It is very appealing to add the lensing dispersion constraint to the likelihood analysis of the PLANCK data. We believe that numerical simulations with initial conditions as suggested here, $\alpha(k_0), \beta(k_0) \neq 0$ which will give a more accurate late time power spectrum will yield similar results, thus strengthening our argument. Last, we have suggested using the (absence of) dispersion to constrain the primordial power spectrum. Since the dispersion depends on several cosmological parameters, it can be useful in constraining other fundamental cosmological parameters as well.

Acknowledgements It is a pleasure to thank Thomas Konstandin, Alexander Westphal and Mathias Zaldarriaga for helpful discussions, comments and suggestions. The work of I.B.-D. is supported by the German Science Foundation (DFG) within the Collaborative Research Center (CRC) 676 Particles, Strings and the Early Universe.

-
- [1] P. Ade et al. (Planck Collaboration) (2013), 1303.5082.
 - [2] J. Bernstein, R. Kessler, S. Kuhlmann, R. Biswas, E. Kovacs, et al., *Astrophys.J.* **753**, 152 (2012), 1111.1969.
 - [3] P. A. Abell et al. (LSST Science Collaborations, LSST Project) (2009), 0912.0201.
 - [4] S. Dodelson and A. Vallinotto, *Phys.Rev.* **D74**, 063515 (2006), astro-ph/0511086.
 - [5] L. Hui and P. B. Greene, *Phys.Rev.* **D73**, 123526 (2006), astro-ph/0512159.
 - [6] I. Ben-Dayan, M. Gasperini, G. Marozzi, F. Nugier, and G. Veneziano, *JCAP* **1306**, 002 (2013), 1302.0740.
 - [7] V. Marra, M. Quartin, and L. Amendola, *Phys. Rev.* **D88**, 063004 (2013), 1304.7689.
 - [8] M. Quartin, V. Marra, and L. Amendola (2013), 1307.1155.
 - [9] M. Kowalski et al. (Supernova Cosmology Project), As-

- trophys.J. **686**, 749 (2008), 0804.4142.
- [10] A. Conley, J. Guy, M. Sullivan, N. Regnault, P. Astier, et al., *Astrophys.J.Suppl.* **192**, 1 (2011), 1104.1443.
 - [11] N. Karpenka, M. March, F. Feroz, and M. Hobson (2012), 1207.3708.
 - [12] T. Kronborg, D. Hardin, J. Guy, P. Astier, C. Balland, et al. (2010), 1002.1249.
 - [13] J. Jonsson, M. Sullivan, I. Hook, S. Basa, R. Carlberg, et al. (2010), 1002.1374.
 - [14] L. Alabidi, K. Kohri, M. Sasaki, and Y. Sendouda, *JCAP* **1305**, 033 (2013), 1303.4519.
 - [15] T. Bringmann, P. Scott, and Y. Akrami, *Phys.Rev.* **D85**, 125027 (2012), 1110.2484.
 - [16] F. Li, A. L. Erickcek, and N. M. Law, *Phys.Rev.* **D86**, 043519 (2012), 1202.1284.
 - [17] J. Chluba, R. Khatri, and R. A. Sunyaev (2012), 1202.0057.
 - [18] J. Chluba, A. L. Erickcek, and I. Ben-Dayan, *Astrophys.J.* **758**, 76 (2012), 1203.2681.
 - [19] J. Chluba and D. Jeong (2013), 1306.5751.
 - [20] A. Kogut, D. Fixsen, D. Chuss, J. Dotson, E. Dwek, et al., *JCAP* **1107**, 025 (2011), 1105.2044.
 - [21] P. Andre et al. (PRISM Collaboration) (2013), 1306.2259.
 - [22] I. Ben-Dayan and T. Kalaydzhyan (to appear).
 - [23] M. Gasperini, G. Marozzi, F. Nugier, and G. Veneziano, *JCAP* **1107**, 008 (2011), 1104.1167.
 - [24] I. Ben-Dayan, M. Gasperini, G. Marozzi, F. Nugier, and G. Veneziano, *JCAP* **1204**, 036 (2012), 1202.1247.
 - [25] I. Ben-Dayan, M. Gasperini, G. Marozzi, F. Nugier, and G. Veneziano, *Phys.Rev.Lett.* **110**, 021301 (2013), 1207.1286.
 - [26] I. Ben-Dayan, G. Marozzi, F. Nugier, and G. Veneziano, *JCAP* **1211**, 045 (2012), 1209.4326.
 - [27] G. Fanizza, M. Gasperini, G. Marozzi, and G. Veneziano (2013), 1308.4935.
 - [28] D. E. Holz and E. V. Linder, *Astrophys.J.* **631**, 678 (2005), astro-ph/0412173.
 - [29] R. Smith et al. (Virgo Consortium), *Mon.Not.Roy.Astron.Soc.* **341**, 1311 (2003), astro-ph/0207664.
 - [30] R. Takahashi, M. Sato, T. Nishimichi, A. Taruya, and M. Oguri, *Astrophys.J.* **761**, 152 (2012), 1208.2701.
 - [31] K. T. Inoue and R. Takahashi, *Mon.Not.Roy.Astron.Soc.* **426**, 2978 (2012), 1207.2139.
 - [32] D. J. Eisenstein and W. Hu, *Astrophys.J.* **496**, 605 (1998), astro-ph/9709112.
 - [33] M. Smith et al. (SDSS Collaboration), *Astrophys.J.* (2013), 1307.2566.